Arch. Metall. Mater. **69** (2024), 3, 1015-1025

DOI: https://doi.org/10.24425/amm.2024.150922

S. KAMATCHISANKARAN[1], A. BOVAS HERBERT BEJAXHIN[2*], K. RAMKUMAR[3], N. RAMANAN[4]

INFLUENCES OF HARDENED ALUMINIUM HMMC ON TRIBOLOGICAL, FLEXURAL AND IMPACT STRENGTH OF WHEEL RIM ELEMENT WITH PROGNOSTICATIONS

The primary goal of this research is to develop hybrid non-ferrous material composites with high flexural and impact strengths by testing the mechanical, thermal, and corrosion properties of AA 6061 wheel rims with various silicon carbide (SiC) and zirconium sulphide ($ZrSO_4$) compositions. This produces an alloy with high strength and perceptible hardenability that is used in a variety of marine space industries. Because of its exceptional strength-to-density ratio, it is a highly sought-after metal matrix composite in the automobile industry. This innovative composite material offers lower weight and higher impact strength when compared to the current wheel rim alloy. Designs of experiments based recommendations and results of simulations in order to prolong the life of the wheel rim.

Keywords: Hybrid composite; Heat treatment; Hardening; Wear test; Wheel Rim; ANSYS

1. Introduction

The properties and structural performance of a composite material, which is composed of two or more chemically distinct and insoluble phases, are superior to those of its constituent parts acting alone. The current market situation establishes the wheel rim market, which focuses on supply and demand analysis, market share, and growth data, as well as contributions from key industry players. The research study provides useful insights on key business strategies. The research below focuses on the composite segment and its application in the current market, including its competitive breadth, opportunities, difficulties, cost, and more. In this segment, we've seen wheel rims with diameters ranging from 10 to 13 inches commercially supplied by a wide range of suppliers, with average weights ranging from 2 to 3.5 kilogrammes, including a 6061 KOSMO Magnesium Series Aluminum rim from Keizer racing. The above all indicates the factors considered for this research paper.

EPFM Dynamic Condition An investigation of a subsurface crack beneath a flat tyre The wheel-flat and a subsurface break in the underside surface were discussed using FEA. They used Elastic-plastic material for the study and calculated the J-Integral factor with a 20° orientation. In comparison to Al_2O_3, the presence of MnS inclusion is more likely to demonstrate a constant increase in J-Integral value, and it can easily produce cracks in the tread of the wheel during the life cycle, as well as aid the crack progress by generating stresses. All the inclusion gives high J-Integral value for an inclined fracture. As the crack depth rises, the J-Integral value falls. [1] As a result, the Hybrid Aluminium Metal Matrix Composite's mechanical characteristics are impacted. On the other hand, hybrid composites contain two or more reinforcements within a single matrix. The research led to the development of Stir Casting-based Hybrid Aluminium Metal Matrix Composites. Hybrid composites with three reinforcements – aluminum oxide (Al_2O_3), silicon carbide (SiC), and boron carbide (B4C) – are created using the base alloy 6061-T6 (Al6061). After that, the cast aluminium metal matrix composites were trimmed to the required sizes in accordance with ASTM guidelines. Tensile, flexural, Charpy impact, and Brinell hardness tests were performed on the created composites to evaluate the effect of reinforcements. A scanning electron microscope (SEM) is used to look at the composites' morphology. The test results were thus reviewed and investigated. We can see that the Hybrid Composites and composites were made using a three-stage mixing procedure and stir casting technique. First sample has the greatest ultimate tensile strength and Young's modulus,

[1] MEENAKSHI SUNDARARAJAN ENGINEERING COLLEGE. DEPARTMENT OF MECHANICAL ENGINEERING, CHENNAI, INDIA
[2] SAVEETHA SCHOOL OF ENGINEERING, DEPARTMENT OF MECHANICAL ENGINEERING SIMATS, CHENNAI, INDIA
[3] DHANALAKSHMI SRINIVASAN UNIVERSITY, SCHOOL OF ENGINEERING AND TECHNOLOGY, TRICHY. INDIA
[4] PSN ENGINEERING COLLEGE, TIRUNELVELI. INDIA

* Corresponding author: herbert.mech2007@gmail.com

according to the tensile test, while second sample comes in second with good findings suggesting high strength. Samples 1 and 2 exhibit high toughness, which means they absorb more energy and fracture more easily, according to the Charpy Impact test. Samples 1 and 3 show higher hardness values than the other two samples, suggesting that they are more resistant to plastic deformation, according to the Brinell Hardness test. [2] Due to the invention of hybrid particle reinforced aluminium alloy metal matrix composite for brake disc production, a typical Honda Accord 2000 model brake disc was manufactured from it. The brake disc's matrix is an aluminium alloy 6061, with reinforcements composed of silicon carbide and coconut shell ash. Utilising stir casting techniques and liquid state manufacturing techniques, composite samples were created. The percentage compositions of silicon carbide and coconut shell ash did not vary, while those of magnesium and graphite did. Magnesium was used to increase wettability by reducing the surface tension of molten aluminium, and graphite was used to improve the tribological characteristics of cast composites. This stir casting machine was specifically created and developed by the authors for this research endeavour. Here, the features and microstructures of the samples were investigated, and the following conclusions were drawn: The composites' microstructure analysis showed that the reinforcing particles were dispersed evenly throughout the matrix. As a result, the bonding qualities were excellent. Magnesium enhances the bonding by increasing the wettability of the reinforcement particles with the aluminium alloy.

[3] The mechanical characteristics and wear behaviour of the silicon carbide and activated carbon-reinforced LM25 aluminium alloy are examined in this study. MMCs have a wide range of technological applications because of their great strength and low weight. The automotive industry employs LM 25 aluminium to make alloy wheels, connecting rods, engine blocks, and engine heads, among other things. The total weight of the LM25 can be decreased while their mechanical qualities can be improved by mixing silicon carbide and activated carbon with them. In this instance, stir casting was employed to make the composite using liquid metallurgy. As a consequence, the tension, compression, wear, and hardness characteristics of the selected composite are contrasted with those of the base metal. The creation of hybrid reinforcement aluminium metal matrix composites is the aim of this effort. An aluminium alloy (LM25) was utilised as the base metal, with silicon carbide in varying weight ratios and 2% activated carbon (AC) as reinforcements, to create a hybrid composite. As a result, the tensile strength of the composite materials increases as the quantity of SiC reinforcements rises. The maximum strength of Al & 2% SiC + 2% AC was determined to be 154 MPa, while the tensile strength of the base metal is 140 MPa. The metal matrix composite's wear rate rises with speed for a given constant load and time. Furthermore, the theoretical densities and the density of cast metal matrix composites are very similar. [4] Numerical calculation and actual confirmation of a radial impact test on an aluminium wheel For vehicle wheels, which are typically subjected to harsh dynamic working conditions, safety is critical. The Severe indoor tests were designed and defined to ensure that vehicle wheels meet the required safety criteria. This research focuses on the analysis and virtual modelling of the radial impact test of aluminium wheels. one of the most demanding tests a wheel must pass before enter manufacturing. For a range of aluminium wheels, the radial impact test is simulated using a finite element model. This model includes the actual tyre structure as well as the wheel, striker, and supporting framework. As a result, the Rayleigh model the parameters of which were established through experimentation is used to account for the Tyre damping. Separate stress/strain curves for the rim and spokes are assigned in order to account for the inhomogeneity non the material of the wheel. As a result, an elasto-plastic isotropic material served as the wheel's representation. It has worked well. The wheel rim and spokes have been given different stress/strain curves in order to take into consideration the material inhomogeneity brought on by the manufacturing of wheels. The interior rim flange residual displacement and maximum impact force were compared to the computer models. Most of the evaluated wheels showed a difference in performance of less than 10% when compared.

[5] Bench testing and simulation study for 90-degree impacts on automotive steel wheels Wheel 90° impact tests with various tyres are also carried out to assess the simulation technique' correctness. The comparison of simulation and test results indicates that distinct tyre effects should be carefully considered in the design of the wheel and that the simulation techniques presented in this study may be useful for determining the impact resistance of the wheel. Impact test at 90 degrees. In some cases, the simplified model may be utilised to design wheel impact resistance and could cut calculation time in half. The inner rim of the wheel exhibits higher deformation than the specified amount (6 mm), according to modelling and bench test findings. This steel wheel does not comply with the standards for a 90-degree collision under the company's configuration. The simulation approach may be used to predict and evaluate whether a wheel will pass or fail a 90-degree impact test. [6] The root source of the flaws was investigated using metallography and sophisticated characterisation techniques. One of the most common causes of surface cracks in wheels is the presence of non-metallic foreign material in the steel. In some circumstances, segregation of components like as carbon and phosphorus in steel sheets has been observed to result in poor material performance during deep drawing or forming at the wheel-end maker's. There is also evidence that a poor shearing procedure at the wheel manufacturer's end can cause wheel cracking. Wheel disc and rim failure was determined to be caused by abnormalities in the mother steel during steel fabrication (casting, rolling), or damages done during the wheel manufacturing process itself, or a combination of both. To avoid the occurrence of the issue, strict quality control is required in all cases, and comprehensive inspection is required to prevent defective components from reaching the final finished product.

[7] An examination of the forging procedure for wheels made of 6061 aluminium alloy, In the simulation, various process settings including punch speed, rim thickness, and die cavity

depth were used. Experiments on a simplified small-scale model were conducted to evaluate the correctness of the formulation used in this work, and they were compared to simulations in terms of forging load. Then, using a full-scale replica of a 6061 aluminium alloy wheel, several procedures were repeated. Material flow, die wall pressure distributions, temperature distributions, and forging loads are among the fundamental pieces of information used in process design and press equipment selection. A comparison of finite element analysis and experimental data in terms of forging load for a simplified small-scale model was used to test the resilience of numerical solutions. Usually, the bottom rim component is constructed first, and then the top rim piece. For minimal load requirements, the bottom rim piece of the die should be open. [8] Design and construction of disc brakes using an aluminium metal matrix composite. AMMC is made of aluminium that has been reinforced with fly ash, a tiny amount of magnesium, and graphite in order to improve the material's chemical, mechanical, and thermal properties. The temperature distribution of the rotor disc is investigated and analysed using FEA analysis, and critical operating temperatures are identified. Cast iron is now utilised for clutches, however it will be replaced by an aluminium metal matrix composite. The strength-to-weight ratio of composite materials is a benefit. According to the findings of the static analysis, the studied stress values were less than the pertinent yield stress values of the aluminium MMC 6061 with 4% fly ash composite. To determine the materials' stresses, theoretical computations were performed on each material. Based on the results, the stress levels were lower than the pertinent permitted stress values for all materials. The stress value was lower in the AA6061 and 4 percent fly ash composite values. As a result of the analytical and theoretical results, it is concluded that the AA6061-4 percent fly ash composite is superior. [9]According to the preceding literature, the most commonly used components are Al 6061, Zricon sand, and SiC. As a result, the compounds were employed in this experiment. [24] AZ31B magnesium alloy's corrosion resistance was enhanced through electrophoretic coating with biocompatible materials, making the surfaces hydrophobic. These coated alloys retained stability in corrosive liquids and simulated body conditions, making them suitable for bio-implants. [25] The study focuses on redesigning the acrylonitrile butadiene styrene water tap flow nozzle aerator for improved flow, discharge, and pressure. It utilizes 3-D printing for precise prototypes and analyzes fluid dynamics with ANSIFLUENT and CFD tools

In this research work, the alloy with high strength and discernible hardenability, this is employed in a range of maritime and space sectors. It is a highly sought-after metal matrix composite in the automotive sector because to its outstanding strength-to-density ratio. When compared to the present wheel rim alloy this novel composite material is lighter and has higher impact strength which can be verified. Experiment designs based on recommendations and simulation findings to extend the life of the wheel rim. The prime aim is to create hybrid nonferrous material composites with high flexural and impact strengths by investigating the mechanical, thermal, and corrosion characteristics of AA 6061 wheel rims with different silicon carbide (SiC) and zirconium sulphide (ZrSO4) compositions

2. Materials and methods

Everything in this world is made up some materials. I may be completely made up of same materials or either combination of different materials. Similarly today's wheel rim are also made up of completely single material or it may be made up of composite materials. The current materials were used in manufacturing of wheel rim are Mg alloy, Forged steel and steel carbon 1008. Each material have their uniqueness in their properties, likewise the most commonly used materials for the wheel are Mg alloy and Al alloy. In these two alloys materials the Al alloy is most commonly used materials for all automobiles. This is because of his light weight and high strength, while compared with the Mg alloy. So in our project we are also using the Al alloy to obtain the light weight and high strength. In fact the Al alloy is used same as the base material but a different series of Al material which is not used in the existing Al material. And similarly the reinforcement materials are also changed and it is selected based upon its strength and high melting point. Since this project is to improve the impact strength and thermal resistance and thereby reduce the stress formed on the wheel rim. So for this we have chosen Aluminium as the base materials and the reinforcement materials was Silicon Carbide and the Zircon sand were used.

3. Fabrication and experimentation

The fabrications of the composite materials were made into three different samples, in which each samples are made of different proportions. The composite materials are Aluminium 6061, Silicon Carbide and the Zirconium sand. In these, the Aluminium 6061 acts as a base material and the other two elements are acts as reinforcement materials. These elements are mixed in three different proportions by using the stir casting. The stir castings are used for the mixing of two or more components to form a molten metal matrix composite (MMC). Hence the three different compositions of the materials are listed in below table.

Fig. 1. Stir casting arrangement

Fig. 2. (a) Tensile test sample of Al6061 HMMC for the load of 40 KN

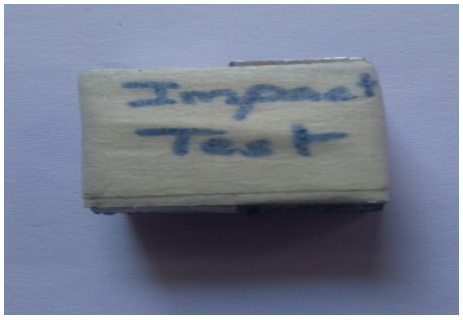

Fig. 2. (b) Impact test sample for the load of 492.95 N

The method followed for the preparation of specimen is Stir casting with motorized operation has been performed. Stir casting is a metal matrix composite manufacturing method that involves stirring a molten metal alloy while introducing solid reinforcement particles, such as ceramics or carbides. This process ensures even distribution of particles within the matrix, resulting in improved material properties, making it commonly used in developing high-performance composite materials.

In these the proportion of the composite materials are chosen based upon the strength of the metal matrix composite under the trial and error method. The chemical composition of Al6061 and SiC is mentioned in the TABLE 1. Once the proportions of the composite have been confirmed then it is said to be casted in the stir casting. The stir casting was explained above.

3.1. Testing of sample

The test sample is the one in which contains only the aluminium 6061 and silicon carbide in required proportions where the zirconium sand is not added for the first sample as mentioned in the TABLE 2. The proportions of the sample 1 contains about 97.5% of Al 6061 and 2.5% of Silicon Carbide. For these samples 1 had been casted and then it is machined for the mechanical testing purposes like Tensile strength, Impact Strength and the Flexural strength. The machined part of the sample 1 for all the three tests are figured below.

3.2. Heat treatment

Heat treatment can be referred to as increase in strength of material, which can also be used to alter the manufacturing objectives such as machining, formability and ductility, due to which the property of the metal is characterised by shape and alignment of atoms which distinguishes the product performance and other desirable characteristics. The practise of heating and cooling metals to modify their microstructure and bring out the physical and mechanical qualities that make metals more appealing is referred to as heat treatment. The heat treatment sample figure is shown below.

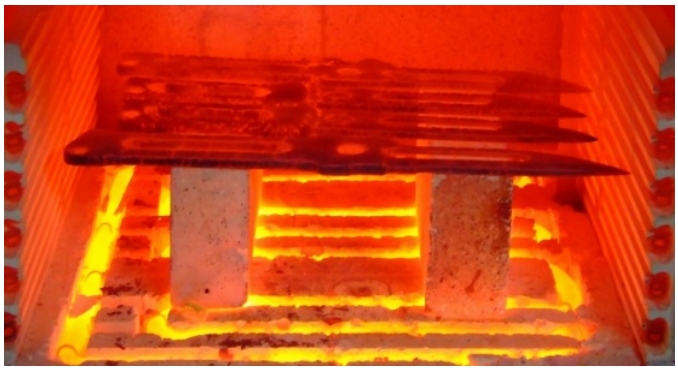

Fig. 3. Heat treatment in a Muffle furnace temp range of 300°C to 1,200°C

TABLE 1

Chemical composition of AA 6061-T6 and SiC

Grade	Al	Cr	Cu	Fe	Mg	Mn	Si	Ti	Zn	Others
65032/Al6061	95.8-98.6	0.04-0.35	0.15-0.4	Max 0.7	0.8-1.2	0.15	0.4-0.8	0.15	0.25	0.20

Grade	Ni	Fe	Al	Ca	C	O	Si	Impurities
SiC	>15	6-10	0.001	0.26	0.001	1.5	99.41	0.1

TABLE 2

Fabrication samples with different compositions

	Sample 1	Sample 2	Sample 3
Al 6061	97.5%	97.5%	95%
SiC	2.5%	0%	2.5%
$ZrSO_4$	0%	2.5%	%

A muffle furnace is a type of laboratory furnace that provides controlled high-temperature environments, typically used for tasks like heating, drying, and heat treatment of materials. The temperature range of a muffle furnace can vary depending on its design and purpose. However, most muffle furnaces offer temperature ranges between 300°C (572°F) to 1,200°C (2,192°F). Some high-end models may even reach higher temperatures,

exceeding 1,500°C (2,732°F). The specific temperature range of a muffle furnace can be determined by the furnace's heating elements, insulation, and control systems. It's important to choose a muffle furnace with a temperature range that suits your intended applications and materials. Always refer to the manufacturer's specifications and operating instructions for the precise temperature range of a particular furnace model.

3.3. Precipitate hardening

Precipitation hardening is a type of age hardening in which heat treatment is used to provide strength to metals and alloys, and the metal is aged by heating or storing it at lower temperatures, allowing precipitates to develop. Precipitation hardening is a method that creates tiny particles of an impurity phase that hinder dislocation movement by controlling variables like temperature and solid solubility. In composite materials that utilise particles as reinforcement, contaminants have the same function as particle substances. Precipitation in solids can result in a broad range of sizes of particles with very diverse qualities; just like ice formation in the air might generate clouds, snow, or hail depending on the temperature history of a specific area of the sky. Contrary to routine tempering, alloys must be maintained at high temperatures for hours to allow precipitation to take place. "Ageing" is the term used to describe this time period. The abbreviation "STA" is frequently used in metals standards and certifications to refer to solution treatment and ageing. The three steps of precipitate hardening that are examined and analysed are tempering, quenching, and ageing is mentioned in TABLE 3.

TABLE 3

Hardening process parameters

Parameters		
Process	**Temperature**	**Durations**
Tempering	565°C	3 hours
Quenching	79°C	25 minutes
Ageing	180°C	6 hours

3.4. Wear measurement

Wear, which results in damage, is the gradual loss or distortion of material from solid surfaces. Wear can be chemical (such as corrosion) or mechanical (such as erosion). The scientific study of wear and related processes is known as tribology. Functional surfaces degrade as a result of wear in machine parts and other processes including fatigue and creep, which finally result in material failure or functionality loss. Metals are prone to wear because surface and near-surface material is displaced by plasticity and wear debris particles are separated. Millimetres to manometers are among the sizes of particles. Contact with non-metallic materials, liquids flowing, solid particles, other metals, or liquid droplets entrained in moving gases can all start this reaction. Numerous factors, such as the kind of loading (impact, static, or dynamic), type of motion (slide, rolling), temperature, and lubrication, in particular the deposition and wear out of the boundary lubrication layer, affect the rate of wear. Numerous wear processes and kinds can be detected depending on the tribo-system.

3.5. Pin on disc wear technique

Here, the pin-on-disc sliding wear test is used to determine the diamond film's coefficient of friction and wear mechanism. Thus the wear which replicates here is the gradual removal or deformation in the solid surface; it means the wear to be mechanical or chemical. From the study we come to know that the wear and its associated process can be referred to tribology. Wear can result from wear on its own, from fatigue and creep, from degradation of the functional surfaces, and lastly from loss of functionality or material breakdown. Thus, variables such as the kind of loading (impact, static, or dynamic), type of motion (slide or rolling), temperature, and lubrication, in particular the deposition and wearing out of the boundary lubrication layer, affect the wear rate. There are several wear kinds and wear processes that depend on the tribo-system. Examples of wear measuring procedures include utilising a precision balance to determine weight (mass) loss, profiling surfaces, or using a microscope to determine the wear depth or cross-sectional area of a wear track to determine where volume loss or linear dimensional change. This equation has a value that is independent of hardness. The sliding distance may be estimated by multiplying the linear speed by the test period. Below is a list of the pins on the disc wear diagram.

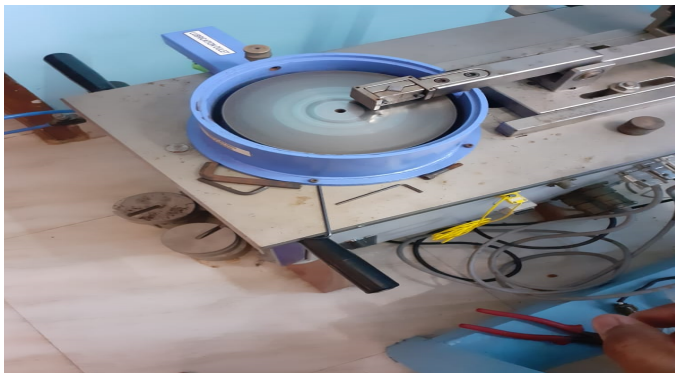

Fig. 4. Arrangement of Pin-On-Disc wear testing machine

3.6. Modelling of a wheel rim

The wheel rim to be modelled for the simulation of stress deformation and stress distribution. So here we have constructed the wheel rim of Bajaj pulsar 150 cc. with the alternation of diameters. The modelling measurements of the wheel rim are listed below.

a) External diameter – 475 mm,
b) Internal diameter – 130 mm,
c) Rim leg length – 107 mm,
d) Rim leg angle – 72°.

The wheel rim's intricate extruded solids are meticulously designed using CATIA, enhancing their quality. Subsequently, this design can be seamlessly integrated into the ANSYS platform in IGES format for comprehensive structural analysis of the wheel rim. In this we have used the CATIA V5 for the modelling and also used the ANSYS workbench. Form this stress deformation can be obtained. The models drawn in the CATIA V5 are shown in the figure. Once the wheel has been modelled it is said to simulated in ANSYS workbench, then by this the load has been tested and also simulated for the stress distribution. From this the finite element analysis method also been used.

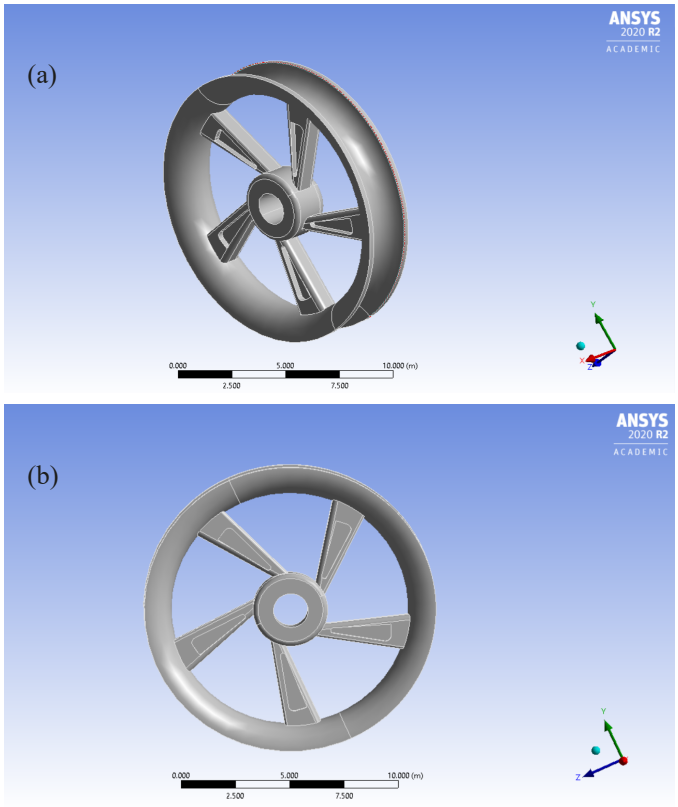

Fig. 5. (a) Three dimensional view of wheel rim (b) Side view cross-section of the wheel rim

From this we can easily able to find the stress distribution on the wheel rim. The circular solid modeling can be made easier the part models using five ribbed structure of the wheel rims. The protected type of flange ends of the wheel rim connected with the ridges instead of using the spokes.

4. Results and discussion

4.1. Tensile test analyses

The tensile test has been conducted for sample 3 of the specimen. For this the tensile test is alone tested because the higher tensile test higher the impact, flexural and wear strength. For this the sample 3 has been machined for three specimens where they are tested after the precipitate hardening. Later that we have found that the three sample 3 have higher tensile strength when they are compared with the above other sample of 1 and 2 as mentioned in Fig. 6(a). That too in sample 3, the specimen 3 has higher tensile strength while compared with the other two specimens of the same sample 3. The graph of the tensile test for the sample 3 has been listed.

TABLE 4

Tensile test of sample results of each specimen

Test Parameter	Observed Values		
Sample ID	**T1**	**T2**	**T3**
Yield strength (N/mm^2)	102	108	117
Ultimate tensile strength (MPa)	124	119	144
% of elongation in 25 mm GL	3.50	4.50	4.50

Thus the table 4 shows the value of the sample 3 for all three specimens. And also it explain the values for the Yield strength, UTS and the Elongation of the specimens, also they are placed in the table to compare the values are shown in the below table.

4.2. Flexural value analysis

The Flexural test values are tested for the both sample 1 and 2 of the specimen which are casted on the proportion listed at the casting procedures. Here the impact values are tested and made an analysis from that, it clearly shows that the sample 1 has high impact value when it is compared with the sample 2. Also the graph of the two samples are also listed from that we can easily analysis the impact value. Consolidated values of tensile, yield strength and percentage of elongation is mentioned in the TABLE 5.

TABLE 5

Observations of Flextural samples test results after and before heat treatments

Testing	Before heat treatment				After heat treatment			
	Sample 1	**Sample 2**	**Sample 3**	**Avg.**	**Sample 1**	**Sample 2**	**Sample 3**	**Avg.**
Tensile strength (MPa)	46.7	58.97	69.97	**58.54**	129.8	139.4	161.98	**143.82**
Yield strength (MPa)	42	58.2	66.2	**55.50**	87.5	94.67	117	**99.59**
Elongation in %	2	2.75	3.22	**2.60**	4.22	5.46	8.9	**6.16**
Flexural load (KN)	4	4.2	5	**4.43**	3.97	6.22	11.4	**7.17**

4.3. Impact Value Analysis

The impact values are tested for the both sample 1 and 2 of the specimen which are casted on the proportion listed at the casting procedures. Here the impact values are tested and made an analysis from that, it clearly shows that the sample 2 has high impact value when it is compared with the sample 1. Also the graph of the two samples are also listed from that we can easily analysis the impact value.

TABLE 6

Impact Results of Sample specimens

Sl. No	Impact test value before heat treatment				Impact value after heat treatment			
Samples	Sample 1	Sample 2	Sample 3	Avg.	Sample 1	Sample 2	Sample 3	Avg.
1	9	13	14	**12**	17	22	27	**22**
2	11	14	17	**14**	21	26	33	**27**
3	11	15	19	**15**	21	28	35	**28**

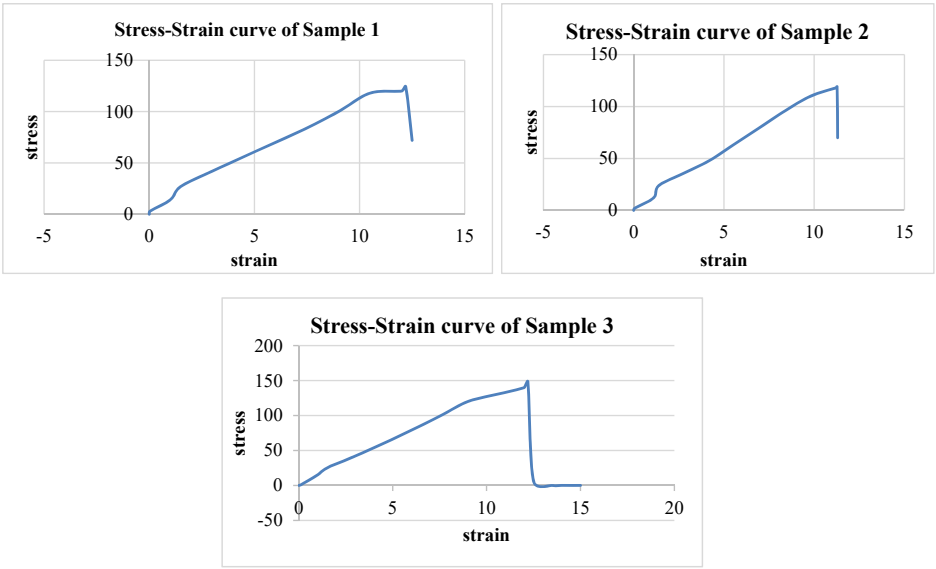

Fig. 6. (a) Stress Strain curves of tensile values of the testing samples 1,2 and 3

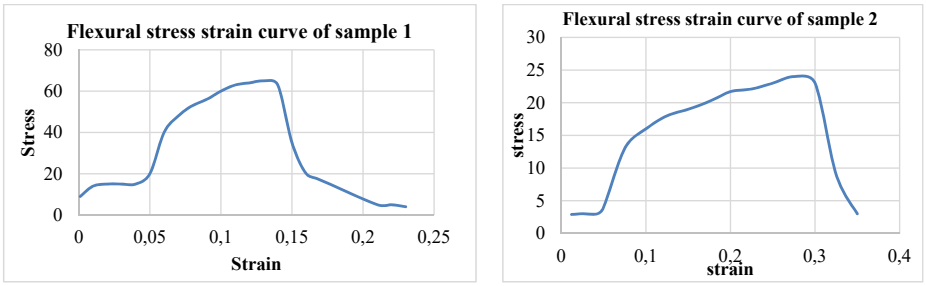

Fig. 6. (b) Flexural values stress-strain curves of Samples 1 and 2

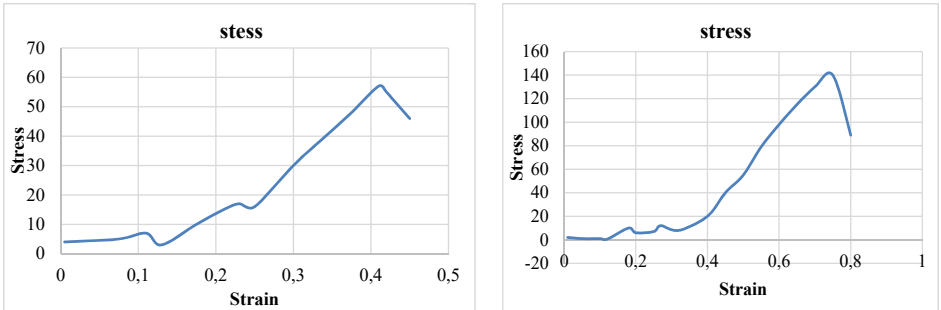

Fig. 6. (c) Impact values stress – strain curves of samples 1 and 2

TABLE 7

Experimental Wear test Results of Hybrid Metal Matrix Composites in Pin on disc apparatus

Sl. No	Sliding Speed in m/s	Sliding Distance, D (m)	Loads L (N)	WR* E-3	SWR* E-3	COF	GRC SWR	GRC WR	GR COF	GR Grade
1	15	1000	15	7.468	0.63	0.465	0.569	0.602	0.621	0.591
2	15	2000	30	3.674	0.136	0.3974	1.01	1	1	1
3	3	1000	30	15.194	0.513	0.4353	0.549	0.233	0.549	0.437
4	3	2000	15	15.74	1.16	0.5954	0.323	0.312	0.343	0.323

All of the designs, graphs, and analyses in this study were made using Minitab statistical software. Fig. 4.1 demonstrates that the GRG reduces as the weight, reinforcement, sliding speed, and distance all rise. When the pin moves over the disc, it first wears, but when a mechanically mixed layer develops, it resists the composite pin's rate of wear. The average of each response characteristic for each factor level is shown in the response table. Based on delta statistics, which assess the size of impacts, the table includes rankings. The delta statistic is the highest minus the lowest average for each element. The rankings show how crucial each element is to the outcome. According to the rankings and delta values, sliding distance, sliding speed, percentage of reinforcement, and load, in that order, have the most effects on GRG. The graph demonstrates that the highest CGG is provided by the two levels of sliding speed, two levels of sliding distance, one level of load, and two levels of reinforcement.

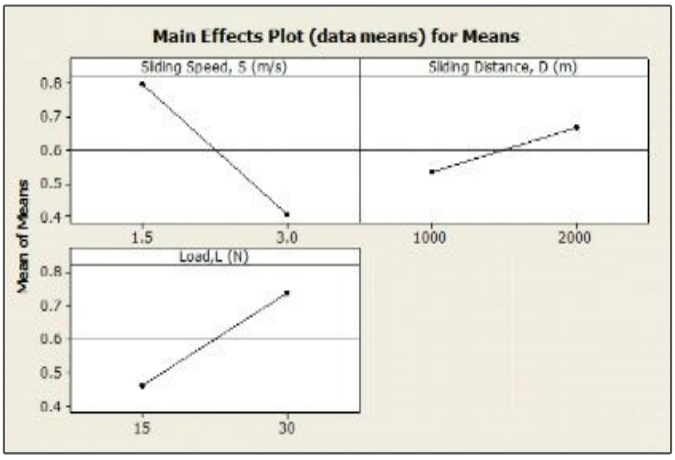

Fig. 7. Main effects plots of sliding speed, distance and load on wear rates

TABLE 8

Response Table for the Hybrid Metal Matrix Composite

Level	Sliding Speed (m/s)	Sliding Distance (m)	Load (N)
1	0.815	0.543	**0.471**
2	**0.406**	0.676	0.748
Delta	0.59	0.679	0.609
Rank	1	2	3

Analysis of variance (ANOVA) was carried out to investigate the importance of the process factors to GRG. We can see from the ANOVA table that the factors of sliding speed and sliding distance had the most influence on achieving the highest GRG, whilst reinforcement and load had less of an impact.

TABLE 9

Anova Table for the Hybrid Metal Matrix Composite

Source	DOF	Sequence Sum of Square	Mean Sum of Square	Contribution
Sliding Speed	1	1319	0.644	36.48%
Sliding Distance	1	1109	0.542	31.33%
Load	1	1197	0.598	33.29%
Total	3			100 %

4.4. Confirmation Experiment

To choose the ideal parameters, the experimental data are examined. According to the response table, the variables at level S2, D2, L2 that are Sliding Speed 1.5 m/s, Sliding Distance 2000 m, Load 30 N, and 5% Aluminium Oxide with reinforcement are the best parameters for attaining the lowest wear rate, specific wear rate, and coefficient of friction. The confirmation experiment and the predictions of the wear rate, specific wear rate, and coefficient of friction are carried out using Taguchi Design of Experiments and the optimal parameters.. The predicted and experimental GRG values were the same, resulting in a value of 1. As a result, the optimization technique is appropriate for this research project. In the composites, the aluminium oxide forms a thin solid lubricant layer. It is lamellar in structure. It guards against wear on composite materials. The optimum level for these composite materials is 5% Al_2O_3 and 2% SiC. Minitab statistical software was used to create all of the designs, plots, and analyses in this study. TABLE 4.2 demonstrates that the GRG reduces as the sliding speed, reinforcement, sliding distance, and load increase. When the pin moves over the disc, it initially wears, but as soon as a mechanically mixed layer formed, it resists the composite pin's rate of wear.

4.5. Simulation results

Thus the simulation result from the ANSYS show the variation in the equivalent stress and the total deformation and their images are shown below. The intensity of stress has been indicated in Fig. 8(a) that the more stress can be observed near

each centre joint of the rim flange. Due to the smaller cross joints in the connected portion of the wheel rim leads to narrow stress intensities. Similarly, the total deformation has been observed more in the outer rim of the wheel structure as shown in Fig. 8(b). It is very less observed at the centre of the wheel rim. This clearly indicates that the more stress can occur due to the narrow geometrical changes as well as the more deformation can occur due to the higher cross section of the wheel rim structure.

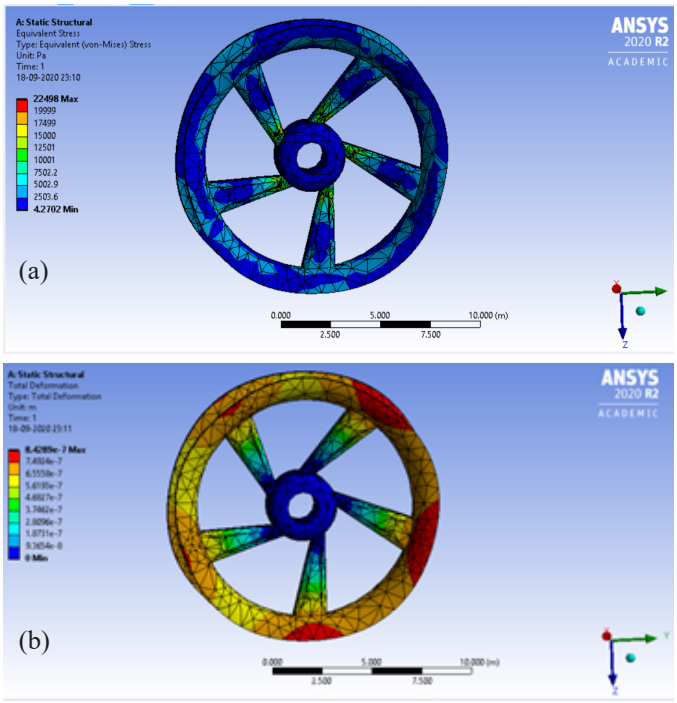

Fig. 8. (a) Stress intensity of the wheel rim and Spokes (b) Total Deformation and equal stress

The brick 8 node element type has been chosen for making the simulation of this wheel rim element which was developed through the extruded solid modelling. The consecutive mesh has been utilized for getting the precise measurement of stresses and strains in each respective node.

The homogenous distribution of the reinforcing phases is the first prerequisite for a composite material to demonstrate its superior performance. The mechanical characteristics of the composite are compromised by the agglomeration of the reinforcing particles. The crucial phase towards a homogenous distribution is the matrix and reinforcement mixing process. The size and form of the particles that make up the matrix and reinforcement also affect the composite's mechanical and physical properties. The well bonded composite structure can reveal the perfect tensile strength and more flexural strength over the tested samples of each composite as shown in Fig. 9.

This reduction in hardness with increasing Zirconium Sulphate concentration may also be linked to the microstructures of composites. As the amount of SiC reinforcement increased, the hardness increased because at high percentages of Silicon and its carbides, the reinforcement particles, which are soft, float in large quantities on the surface of the molten aluminium, causing

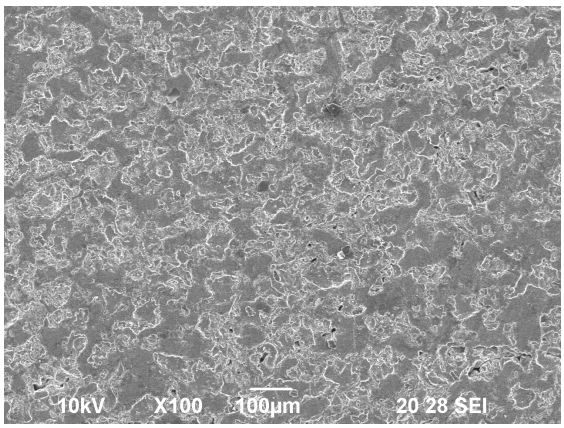

Fig. 9. SEM image of Al6061-SiC-$ZrSO_4$ Hybrid Metal Matrix Composite

the reinforced effect to increase, thereby elevating the hardness. In the microstructure, it was observed that SiC and Zr particles are prevalent in a very small area, each with a weight percentage of 2.5% which is observed from Fig. 10.

The chemical compositions of ferrous and non-ferrous materials often affect how they behave physically. The majority of elements found in all materials have the potential to influence an alloy's or a composite's properties. In this situation, the involvement of silicon and zirconium particles may help the composites' matrix structural bonding. With the abundance of ductile nature, the SiC addition mostly aids in raising the hardness and tensile strength. The strongest heat-treatable aluminium alloys are made when zirconium sulphate is added to aluminium along with a few additional components. The addition of Zr significantly boosts flexural strength and allows for precipitation hardening. Therefore, the incorporation of heat treatments may disclose the robust and dynamic material features among all composites.

5. Conclusion

After all analysis made and simulated in ANSYS 2020 R2, the stress, strain, load impact of the wheel rim were analysed. By this we have concluded that our design, the material and their composition we have chosen are correct. And we have found that the newly made composite material have more yield strength, impact strength and also the wear value are also increased. And thereby, the elongations of the material are reduced. In addition to that the life time of the wheel rim has increased while compared to the existing one. The highlighted aspect was the achievement of a sliding speed resulting in a 36.48% reduction in wear rate. Impact strength ranged from 27 to 35J, while tensile strength fell between 139.4MPa and 161.3MPa, with a yield strength of 117MPa. Sample 3, containing 2.5% SiC and ZrSO4, notably enhanced these mechanical properties, including impact strength and wear rate. Thus it has been verified with the SEM micrographs which contain more strain hardened matrix casted material structure. It has well bonded structure due to precipitation hardening used to deliver better mechanical properties.

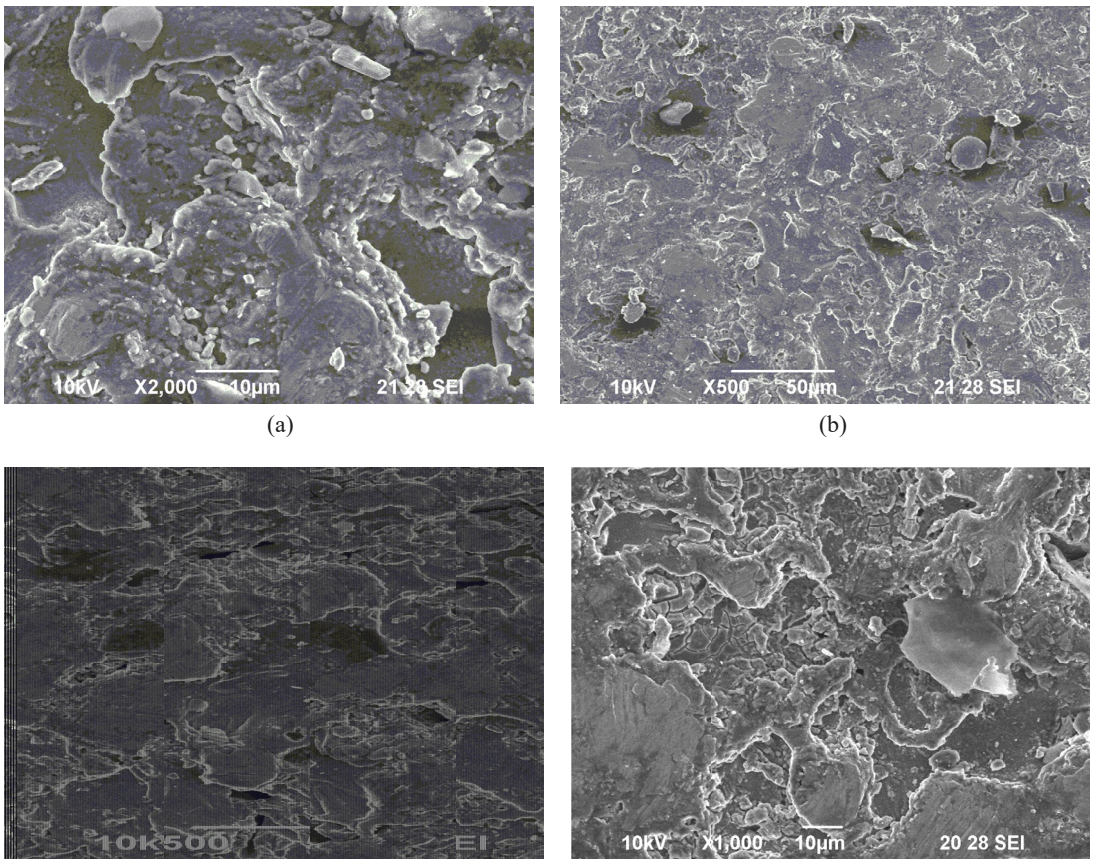

(a) (b)

(c) (d)

Fig. 10. (a) Homogeneous structure of Al-SiC-$ZrSO_4$ Metal Matrix Composite; (b) Particulate dispersion of 2.5% of $ZrSO_4$; (c) Distribution of Silicon particles in to Al6061; (d) Al6061-SiC Metal Matrix Composite without $ZrSO_4$

REFERENCES

[1] Nagavendra Kumarkanoje, Sathish C. Sharma, S.P. Harsha, EPFM Analysis of Subsurface Crack Beneath a Wheel Flat Using Dynamic Condition. Science Direct Proced. Matl. Sci. **6**, 43-60 (2014).

[2] A.T. Alpas, Sandeep Bhattacharya, lan M.Hutching, Wear of Particulate Metal Matrix Composites Science direct. Compr. Comp. Matl II, **4**, 137-172 (2018).

[3] Moona, Girija, R. Walia,Vikas, Rastogi, Sharma, Rina, Parametric optimization of fatigue behaviour of hybrid aluminium metal matrix composites. Matl.-today: Proceedings **21**, (2019). DOI: https://doi.org/10.1016/j.matpr.2019.10.002

[4] P. Sriram Murthy, Y. Seetha Ram Rao, Impact on Mechanical Properties of Hybrid Aluminium Metal Matrix Composite. Int. Jour. of Engg. and Adv. Tech. (IJEAT) **8** (6), 1638-1645 (2019). ISSN: 2249-8958.

[5] Justine Osange, Akaindapo, Jacob Olaitan, Development of Hybrid particle reinforced aluminium alloy metal matrix composite for the production of Break disc. Amer. Jour. of Engg. Research (AJER) **8** (9), 88-97 (2019). e-ISSN 2320-0847 p-ISSN 2320-0936

[6] S. Patil, R.Robinson, B.P. Madhu, G.Manjunath, M.Kalyana Kumar, Investigation of Mechanical properties and Wear behaviour of Lm 25 aluminium alloy reinforced with silicone carbide and Activated carbon, Int. Jour. of Research and Sci. Innov. (IJRSI) **5** (1), (2018). ISSN 2321-2705

[7] G. Previati, F. Ballo, M. Gobbi, G. Mastinu, Radial impact test of aluminium Wheel – Numerical simulation and experimental validation. Int. Jour. of Impact Engg. Science Direct **126**, 117-134 (2019).

[8] Choongdo Lee, Science direct, Effect of Strain rate on fatigue property of A356 aluminium casting alloys. Jour. of Mat. Engg. and Perf. **31** (2), 1-11 (2021). DOI: https://doi.org/10.1007/s11665-021-06297-9

[9] Qian Gao, Yingchun Shan, Xiaofei Wan, Qizhang Feng, Xiandong Liu, 90 – degree impact bench test and simulation analysis of automotive steel wheel. Engineering Failure Analysis, Science Direct **105**, 143-155 (2019).

[10] Dey, Arthita, Jugade, Hrishikesh, Jain, Vaibav, Adhikary, Manashi, Cracking phenomena in automotive wheels: An insight. Engg Fail. Analysis. **105** (2019). DOI: https://doi.org/10.1016/j.engfailanal.2019.01.069

[11] Y.H. Kim, T.K. Ryou, H.J. Choi, B.B. Hwang, An analysis of forging process for 6061 aluminium alloy wheels. Science direct, Jour. of Matl. Process. Tech. **123**, 270-276 (2002).

[12] G. Ganesan, S.Magibalan, S.Gokul, K.P.Gopalakrishnan, S.Packiyaraj, Design and Fabrication of Disc brake by using aluminium metal matrix composite. Jour. of Engg. Tech. and Innov. Research (JETIR) **4** (4) (2017). ISSN 2349-5162

[13] Shipra Verma, P.Sudhakar Rao, Study of Mechanical behaviour of Aluminium 6061 Alloy based composite review. Jour. of Mech.

and Civil. Engg. (IOSR – JMCE) **15** (4), V.3, 16-20 (2018). e-ISSN 2278-1684, p-ISSN 2320-334X.

[14] Lei Chen, Shunping Li, Huiqin Chen, David M Salyor, Shuiguang Tong, Study on the design method of equal strength rim based on stress and fatigue analysis using Finite element analysis method. Advances in Mechanical Engineering **9** (3), 11 (2017).

[15] P. Sureshkumar, T. Jagadeesha, L. Natrayan, M. Ravichadran, Dhinakaran Veeman, S.M. Muthu. Electrochemical corrosion and tribological behaviour of AA6063/Si3N4/Cu $(NO3)_2$ Composite processed using single-pass ECAPA route with 120° die angle. Jour. of Matr. Research and Tech. **16**, 715-733 (2022).

[16] L. Natrayan, M. Senthil Kumar, A novel feeding technique in squeeze casting to improve the reinforcement mixing ratio. Mater. Today Proc. **46**, 1335-1340 (2021).

[17] S.M. Sivagami, A. Bovas Herbert Bejaxhin, R. Gayathri, T. Raja Vijay, K. Punitharani, P. Keerthi Vasan, M. Meignanamoorthy, On the Selection of a Composite Material for Two-Wheeler Foot Bracket Failure Prevention through Simulation and Mathematical Modeling. FDMP **18** (3), (2022).
DOI: https://doi.org/10.32604/fdmp.2022.018752

[18] Vasudeva Rao, P. Periyaswamy, A. Bovas Herbert Bejaxhin, E. Naveen, N. Ramanan, and Aklilu Teklemariam, Wear Behavioural Study of Hexagonal Boron Nitride and Cubic Boron Nitride-Reinforced Aluminum MMC with Sample Analysis, Hindawi, Journal of Nanomaterials. Article ID 7816372, 10 pages (2022).
DOI: https://doi.org/10.1155/2022/7816372

[19] N. Muthu Mekala, C. Balamurugan, A. Bovas Herbert Bejaxhin, Deform 3D Simulation and Experimental Investigation of Fixtures with Support Heads". Mechanika **28** (2), 130-138 (2022).
DOI: http://dx.doi.org/10.5755/j02.mech.29468

[20] A. Bovas Herbert Bejaxhin, G.M. Balamurugan, S.M. Sivagami, K. Ramkumar, V. Vijayan, S. Rajkumar, Tribological Behavior and Analysis on Surface Roughness of CNC Milled Dual Heat Treated Al6061 Composites. Advances in Materials Science and Engineering, Article ID 3844194, 14 (2021).
DOI: https://doi.org/10.1155/2021/3844194

[21] V.P. Srinivasan, Ch. Sandeep, C. Shanthi, A. Bovas Herbert Bejaxhin, R. Anandan, M. Abisha Meji, Comparative Study on EDM Parameter Optimization for Adsorbed Si3N4–TiN using TOPSIS and Coupled with TLBO Algorithm. Abso. Sci. & Technology, Article ID 4112448, 19 (2022).
DOI: https://doi.org/10.1155/2022/4112448

[22] Y. Brucely, Y.C. Shaji, A.B.H. Bejaxhin, M. Abeens, Online acoustic emission measurement of tensile strength and wear rate for AA8011-TiC-ZrB2 hybrid composite. Surface Topography: Metrology and Properties **10** (4), 045009 (2022).

[23] C.B. Priya, K. Ramkumar, V. Vijayan , A. Bovas Herbert Bejaxhin, Wear Studies on Mg-5Sn-3Zn-1Mn-xSi Alloy and Parameters Optimization Using the Integrated RSM-GRGA Method. Silicon **15**, 3569-3579 (2023).
DOI: https://doi.org/10.1007/s12633-022-02243-z

[24] H. Koten, O. Kamaci, (2023). Time-Dependent Corrosion Resistance Investigation of Hydrophobic Magnesium Alloys. In: Emamian, S.S., Awang, M., Razak, J.A., Masset, P.J. (eds) Advances in Material Science and Engineering. Lecture Notes in Mechanical Engineering. Springer, Singapore.
DOI: https://doi.org/10.1007/978-981-19-3307-3_24

[25] A. Bovas Herbert Bejaxhin, R.B. Rayappa, H. Koten, R. Balasubramanian, D.U. Sarwe, Comparative Design and CFD Analysis of 3-D Printed Acrylonitrile Butadiene Styrene Nozzle Aerator for Discharge Reduction. Thermal Science **26** (2), 857-869 (2022).